PAPER

Bone repair of critical-sized defects in Wistar rats treated with autogenic, allogenic or xenogenic bone grafts alone or in combination with natural latex fraction F1

Biomedical Materials

PAPER

Bone repair of critical-sized defects in Wistar rats treated with autogenic, allogenic or xenogenic bone grafts alone or in combination with natural latex fraction F1

RECEIVED
22 June 2017

REVISED
27 September 2017

ACCEPTED FOR PUBLICATION
20 October 2017

PUBLISHED
8 February 2018

Bruna Gabriela Santos Kotake[1], **Miliane Gonçalves Gonzaga**[1], **Joaquim Coutinho-Netto**[1], **Edilson Ervolino**[2], **Fellipe A T de Figueiredo**[1] and **João Paulo Mardegan Issa**[1,3]

[1] School of Medicine of Ribeirao Preto—University of Sao Paulo, Ribeirao Preto, Sao Paulo, Brazil
[2] Sao Paulo State University Júlio de Mesquita Filho—Araçatuba, Sao Paulo, Brazil
[3] School of Dentistry of Ribeirão Preto, University of Sao Paulo, Ribeirao Preto, Sao Paulo, Brazil

E-mail: jpmissa@forp.usp.br

Keywords: *Hevea brasiliensis*, bone grafts, stereology, zymography, immunohistochemistry

Abstract

Bone grafts are used in the medical-surgical field for anatomical and functional reconstruction of lost bone areas, aiding the bone repair process by osteogenesis, osteinduction and osteoconduction. New materials such as F1 (fraction 1) protein extracted from the rubber tree *Hevea brasiliensis* have been investigated and currently present important properties for tissue repair, and are associated with neoangiogenesis, promoting cell adhesion and extracellular matrix formation. The main objective of this study was to investigate the association of F1 protein to different bone grafts in the repair of critical bone defects in the calvaria of Wistar rats. A total of 112 Wistar rats were divided as follows: autograft (AuG), allograft (AlG), xenograft (XeG), autograft/F1 (AuG–F1), allograft/F1 (AlG–F1), xenograft/F1 (XeG–F1), F1 (F1), control (CTL), with a waiting period of 4 and 6 weeks (w). The stereological AuG, AlG, AuG–F1 and AlG–F1 results had greater bone neoformation ($p < 0.05$). For immunohistochemistry, the angiogenic and osteogenic factors were higher for AuG–F1 and AlG–F1. TRAP-positive cells were higher in XeG–F1 and AlG (37 ± 9.53, 13.3 ± 4.16) (4 w) and XeG, AlG–F1 and XeG–F1 (20.33 ± 7.37; 15.25 ± 6.02, 19.33 ± 3.21) (6 w). For zymography, F1 showed increased gelatinolytic activity of MMP-2 and -9. It was concluded that the bone graft associated or not with F1 increases the angiogenic and osteogenic, biochemical and stereological factors.

1. Introduction

The uses and applications of bone grafts in the medical-surgical field have enabled the anatomical and functional reconstruction of a bone site lost due to congenital or acquired causes, and therefore are of fundamental importance to a patient affected by these diseases. Thus, when applied in a certain location, they promote bone formation in three ways: osteogenesis, osteoinduction and osteoconductivity [1]. There are different types of osseous grafts, such as autogenous, allogenous and xenogenous bone. Autogenous is bone that has the closest standard ideal for bone reconstruction, but is often difficult to obtain due to anatomical limitations of the bone donor site [2].

Considering the numerous options now available to carry out bone grafting, certain features are necessary for the proper selection of the material, namely: potential osteogenesis, osteoconduction and osteoinduction; stability of grafting; does not represent a facilitator of infectious processes; easy accessibility; inexpensive; and does not promote morbidity [3].

Besides bone grafts, new materials have been reported in the literature with the potential recovery of tissues, for example, natural latex extracted from *Hevea brasiliensis* [4–7]. Latex is a substance already described in the literature and has been used extensively in the industry for the production of clinical-surgical supplies in medical and dental fields, but with few studies on experimental animals.

Biomembrane fraction 1 (F1) obtained from latex is made by hand from latex extracted from the *Hevea brasiliensis* rubber tree. Warmed at 60 °C in a stove for polymerization, it is coated with polylysine, a poly-cation

that increases the permeability of vascular and microvascular flow. F1 presents important biological properties *in vivo* in different species such as rats, mice, rabbits, dogs, and humans, demonstrating the ability for neoangiogenesis activity, cell adhesion promotion and extracellular matrix formation [8, 9].

The current literature correlates with this material as a source of allergenic proteins responsible for triggering allergic reactions, especially in health professionals who are constantly exposed to latex used in the manufacture of disposable gloves, in patients with spina bifida, workers at latex factories, and people allergic to banana, avocado, kiwi, chestnut and papaya [10–14]. However, the latex membrane has proved to be efficient, safe and does not cause hypersensitivity reactions in the repair of different tissues [15–19] because, according to Frade *et al* [16], the preparation of the biomembrane at 60 °C does not release the peptide allergens responsible for allergic reactions that may occur in the manufacture of gloves.

Important properties in tissue regeneration have been attributed to F1. These proteins have been shown to be biocompatible, increase angiogenic activity [4] and stimulate bone formation [7], presenting great potential for clinical application. The main objective of this study was to investigate the association of F1 protein to different bone grafts in the repair of critical bone defects in the calvaria of Wistar rats.

2. Materials and methods

2.1. Protein preparation

Serum preparation from fresh natural latex was obtained from the *Hevea brasiliensis* tree obtained from Sao Jose do Rio Preto forest (Sao Jose do Rio Preto, SP, Brazil). The natural latex was treated with NH_4OH (2%) and mixed with a solution of acetic acid 2.2% v/v in a ratio of 1:2. After coagulation, the serum was separated from the rubber and subjected to dialysis and lyophilization. The F1 of the latex was dissolved in a proportion of 1:1 in a neutral solution, represented here by phosphate buffer solution at pH 7.2. It was applied at a concentration of 5 μg with the aid of a previously calibrated micropipette over the desired area [20].

2.2. Animals

A total of 112 male albino Wistar rats were selected, aged 8 weeks, weighing approximately 250 grams, and obtained from the Central Animal Facility of the Campus of Ribeirão Preto, USP. The study was approved by the Ethics Council on animal use of the School of Medicine of Ribeirao Preto, Ribeirao Preto, Sao Paulo, Brazil (Protocol number: 099/2010). The animals were divided into 8 groups, each with a delay until sacrifice at 4 and 6 weeks, totaling 16 groups with 7 animals per group. The animals were housed in boxes of five animals each, with free access to food and water, under controlled temperature conditions (23 ± 1 °C) and a light/dark cycle of 12/12 h, with the beginning of the light period being 07:00 h. The induction of death was started by deep anesthesia followed by decapitation. This method was certificated by the local ethics committee that follows the international laws for animal use.

The groups were divided into:

AuG group: autograft bone

AlG group: allograft bone

XeG group: xenograft bone (lyophilized bovine bone of 300–425 μm, Lumina Bone Criteria, Sao Carlos, Brazil)

AuG–F1 group: particulate autograft +5 μg F1

AlG–F1 group: particulate allograft +5 μg F1

XeG–F1 group: xenograft (lyophilized bovine bone) +5 μg F1

F1 group: 5 μg F1

CTL group: surgical bone defect/control

2.3. Surgical technique

The animals were intramuscularly anesthetized with an anesthetic solution of xylazine (75–100 mg kg^{-1}) and ketamine (5–10 mg kg^{-1}) provided by Agibrands of Brazil LTDA- Campinas, SP, Brazil, and subjected to a sagittal incision in the central calvarial region; the skin was peeled away and the periosteum removed. The critical bone defect in the left and right parietal lobe was performed using a 5 mm internal diameter trephine, adapted to a contra-angle surgical hand piece (Kavo, São Paulo, Brazil) and coupled to an electric motor for implants, set to 3000 rpm and irrigated with abundant saline solution. Each bone defect was filled with 23 mm^3 of bone graft. This diameter of bone defect was adopted, taking as reference other previously published works regarding critical bone defects that cannot be repaired spontaneously [21].

In the immediate postoperative period, all animals received 0.2 ml of penicillin G-benzathine (pentabiotic for veterinarian use in small animals, Forte Dodge Saude Animal Ltda., Campinas, SP).

2.4. Histological processing

After 4- and 6-week periods from surgical intervention, the animals were euthanized, the calvaria was removed and fixed for 24 h in 4% buffered formalin and then decalcified in EDTA 10% for approximately 2 months. After this period, the pieces passed through a diaphanization process, being dehydrated in ascending series of alcohol: 70%, 90%, 95%, 100% (I, II and III). Subsequently, these bone blocks were placed in equal parts of alcohol and xylene and diaphanized in xylene with changes every hour in each solution, with three exchanges performed before finally embedding in paraffin. For microscopic analysis, 5 μm thick semi-serial sections were selected, and these sections were stained with H&E (hematoxylin-eosin) and analyzed using an AxioImager Z2 optical microscope (Zeiss,

Oberkochen, Germany) coupled to a digital camera (Zeiss, Oberkochen, Germany). Before the histological analyses (immunohistochemical and stereological) the samples were codified so that only one researcher knew which groups they belonged to. Later, the analyses were performed by another experienced and calibrated examiner who was not aware of the analyzed groups.

2.5. Quantitative histology–stereological analysis

To quantify the volume of newly formed bone (mm^3), 16 histological sections were randomly selected along the bone defect by an examiner expert in bone biology. These sections were analyzed at 20x magnification and stereological StereoInvestigator software (MBF, USA) was used for this measurement in which the program allows analysis of the tissue volume by the Cavalieri method of estimating neoformation through the application of a test system composed of 150 μm sized grids over the edge of the area of interest. The results were obtained through the sum of the points of the test system over the demarcated new bone tissue area with a thickness of 5 μm. Data were statistically analyzed using the ANOVA and Tukey post test, presenting as mean and standard deviation.

2.6. Immunohistochemical analysis

The histological sections were deparaffinized in xylene and hydrated in descending ethanol series (100°–100°–100°–90°–70° GL). Antigen retrieval was performed in Diva Decloaker® buffer (Biocare Medical, CA, USA) in a pressurized Decloaking Chamber® (Biocare Medical, CA, USA) at 95 °C for 10 min. After washing with phosphate buffered saline solution (PBS) 0.1 M at pH 7.4, the histological slides were immersed in 3% hydrogen peroxide for 1 h. Subsequently, the histological sections were treated with 3% bovine albumin serum for 12 h. Histological slides containing samples from all experimental groups were subjected to incubation with one of the following primary antibodies (Santa Cruz Biotechnology, CA, USA): anti-OCN (osteocalcin) of rat generated in goat (1:100), anti-OPN (osteopontin) of rat generated in goat (1:100), anti-CD31 of rat generated in rabbit (1:180), anti-VEGF of rat generated in rabbit (1:100), anti-VEGF-R2 of rat generated in rabbit (1:100), anti-BMP-2 of rat generated in rabbit (1:100), and anti-TRAP of rat generated in goat (1:100). Primary antibodies were diluted in PBS plus 0.1% Triton X-100 (PBS-TX) for 24 h in a humid chamber. In subsequent steps, we used the Universal Labeled Dako (horseradish peroxidase (HRP)) Streptavidin-Biotin Kit ® (Dako Laboratories, CA, USA). After washing, the histological sections were incubated in biotinylated secondary antibody for 2 h, washed, and treated with streptavidin conjugated with HRP for 1 h. After three washes in PBS-TX the sections were revealed using chromogen 3,3′-diaminobenzidine tetrahydrochloride (DAB Chromogen Kit®, Dako Laboratories, CA, USA). At the end of the series of washes in PBS, the histological sections were counterstained with Harris hematoxylin. As a negative control, the specimens were submitted to the procedures described above suppressing the use of primary antibodies.

2.7. Analysis of the samples submitted to immunoperoxidase

Histological sections were analyzed under a bright field illumination optical microscope (Optiphot-2, Nikon, Japan) by an investigator blind to the experimental groups that were being analyzed. Immunostaining was defined as a brownish presence in the cytoplasm of cells and/or extracellular matrix. In each animal, the entire length of the defective bone was analyzed with 100x magnification. A semi-quantitative analysis was performed using five histological sections of each animal, and the immunostaining pattern was attributed a score. The criterion for the establishment of the scores was adopted from those established by Faria *et al* (2008) [22] with some modification, where 0 = absence of immunostaining, 1 = low standard of immunostaining, 2 = moderate standard of immunostaining, 3 = high standard of immunostaining, 4 = extremely high standard of immunostaining. The data were statistically analyzed using the Kruskal Wallis and Dunn's post test, presented as mean and standard deviation.

2.8. Zymography in SDS-polyacrylamide 12% gel with gelatin substrate to determine the levels of MMP-2 and MMP-9

Metalloproteins (MMPs) were separated by molecular weight by polyacrylamide gel electrophoresis under denaturing conditions. Subsequently, the enzymes were restructured and the proteolytic activity of each isoform was visualized in stained zymograms. First, samples were prepared according to the technique developed and designed for studies using rat bones. The pistil was manually operated and a mean of ten cycles was used. After the pistil was pressed against the bottom grinder, a 90-degree twist to the right was then applied. Thereafter, a piece at the bottom of the grinder was taken out in which the ground bone was deposited. This crushed bone was then weighed and homogenized in extraction buffer (300 μl for each 0.1 g sample) containing 10 mM $CaCl_2$, 50 mM Tris-HCl pH 7.4, 0.1% Brij, 0.15 M NaCl, 1 mM Phe (1:10 ortho phenanthroline), 1 mM phenylmethylsulfonyl fluoride, and 1 mM N ethylmaleimide. It was stored on ice in a refrigerator for 20 h and then centrifuged at 10 000 g for 15 min. The protein content was measured using the Bradford method (Bradford 1976). Subsequently, the samples were diluted 1:1 with sample buffer (final concentration: 2% sodium dodecyl sulfate (SDS), 125 mM Tris-HCl pH 6.8, 10% glycerol and 0.001% bromophenol blue) and placed

for electrophoresis on an SDS-12% polyacrylamide gel, co-polymerized with gelatin (0.1%) as substrate.

After completion of the electrophoresis, the gel was incubated for 1 h at room temperature in Triton X-100 2% solution, and then incubated for 16 h at 37 °C in Tris-HCl pH 7.4 buffer containing 10 mmol L^{-1} CaCl2. The gels were stained with 0.05% Coomassie brilliant blue G-250 and de-stained with 30% methanol and 10% acetic acid. The gelatinase activity was detected through the bands not stained in Coomassie stained gelatin. Enzymatic activity was analyzed by densitometry using the 'Kodak Electrophoresis Documentation and Analysis System 290' (Kodak, Rochester, NY). The gelatinase activity was normalized to internal standard (fetal bovine serum) to enable full and comparative analysis. MMP-2 isoforms were identified in the 72 and 64 kDa bands, and MMP-9 in the 82 and 92 kDa bands. The images were analyzed using GeneTools software (Syngene, Cambridge, UK).

2.9. Statistical analysis

Data from the immunohistochemical analysis were submitted to non-parametric Kruskal–Wallis statistical tests (for group and time factors) and Dunn's test (for comparative analysis) for stereological analysis of new bone tissue (volume), zymography, and immunohistochemical analysis for TRAP using a parametric test, ANOVA and Tukey test. The statistical program used was GraphPad Prism 5 adopting the level of significance of 95%.

3. Results

3.1. Qualitative histological analysis

The CTL showed similar histological characteristics after 4 or 6 weeks postoperative. The presence of an extremely narrow band of new bone tissue exclusive to the edges of the surgical wound was found. Almost all of the bone defect was depicted as filled by connective tissue presenting a large amount of collagen fibers oriented parallel to the surface of the wound, with the presence of moderate amounts of fibroblasts, blood vessels and few inflammatory cells (figures 1(A), (C), 2(A), (C)).

In F1 there was a similarity between the structural characteristics exhibited by the surgical wound after 4 and 6 weeks postoperatively. In most specimens, the new bone was occupied by 1/3 of the surgical wound. The bone strands directed to the center of the bone defect showed themselves to be composed of a delicate network of immature bone trabeculae circumscribed by large medullary spaces. The remaining bone defect was shown to be occupied by well-structured connective tissue. This tissue was comprised of a large amount of collagen fibers, among which were a moderate amount of fibroblasts and many blood vessels.

Tissue responses of AuG (figures 1(I), 2(I)), AlG (figures 1(J), 2(J)), AuG–F1 (figures 1(B), (D), 2(B), (D)), and AlG–F1 (figures 1(E), (G), 2(E), (G)) were similar at 4 and 6 weeks; however, the superiority of the combination of autograft with F1 was clear, where the advancement of bone neoformation was substantially greater. In these groups, the presence of organized bone tissue was found with few bone marrow spaces and trabeculae advancing completely to the center of the defect in most specimens. The center of the bone defect was shown occupied by connective tissue that housed the remaining bone graft particles. On the surface of the majority, the bone apposition of a layer of immature bone tissue was observed, thicker in the specimens at 6 weeks in all groups. Some faces of the particles of the remaining grafts showed no bone apposition, but resorption lacunae occupied by osteoclast assets. A fibrous connective tissue occupied the surfaces of the bone defect and circumscribed the remaining bone graft particles. This tissue consisted of a large amount of collagen fibers, among which was an absence of a moderate amount of fibroblasts, many blood vessels, and rare isolated inflammatory cell outbreaks, especially where bone resorption of the particles of the grafts was actively taking place.

XeG (figure 1(K), 2(K)) and XeG–F1 (figures 1(H), 2(H)) were similar at 4 and 6 weeks. These groups showed both patterns of bone neoformation, which contributed to the new bone formation and occupied much of the extent of the surgical wound, especially after 6 weeks postoperative. There was little display of bone tissue on the remnants of the grafts after 4 weeks postoperative. In this time period, the bone resorption process on the surface of the grafts predominated. After 6 weeks postoperative, there was a greater amount of bone apposition sites, especially in XeG–F1. An intensely vascularized connective tissue covered the surfaces of the surgical wound and the surrounding areas of the remaining bone graft particles. This tissue consisted of a large amount of collagen fibers, among which was observed a moderate amount of fibroblasts and inflammatory cells.

3.2. Quantitative histological analysis

3.2.1. 4-week period

The results demonstrated that AuG (32.12 ± 6.18), AlG (34.71 ± 8.69), AuG–F1 (31.69 ± 2.48), AlG–F1 (32.54 ± 17.95), increased bone neoformation, presenting a statistical difference from the control (11.42 ± 0.27) with a minimum of $p < 0.05$. The other groups did not differ statistically between themselves and the control; however, although not statistically different, these groups showed increased bone formation (figure 3(A)).

3.2.2. 6-week period

Data showed that the AuG (34.02 ± 5.18) and AlG (32.49 ± 9.02), and XeG (33.54 ± 8.94) and XeG–F1 (35 ± 3.47) grafts increased bone neoformation, showing $p < 0.05$ compared to the control (14.02 ± 2.29); the AuG–F1 (49.65 ± 14.34) and AlG–F1 (41.17 ± 6.31) groups increased neoformation with $p < 0.001$. The F1

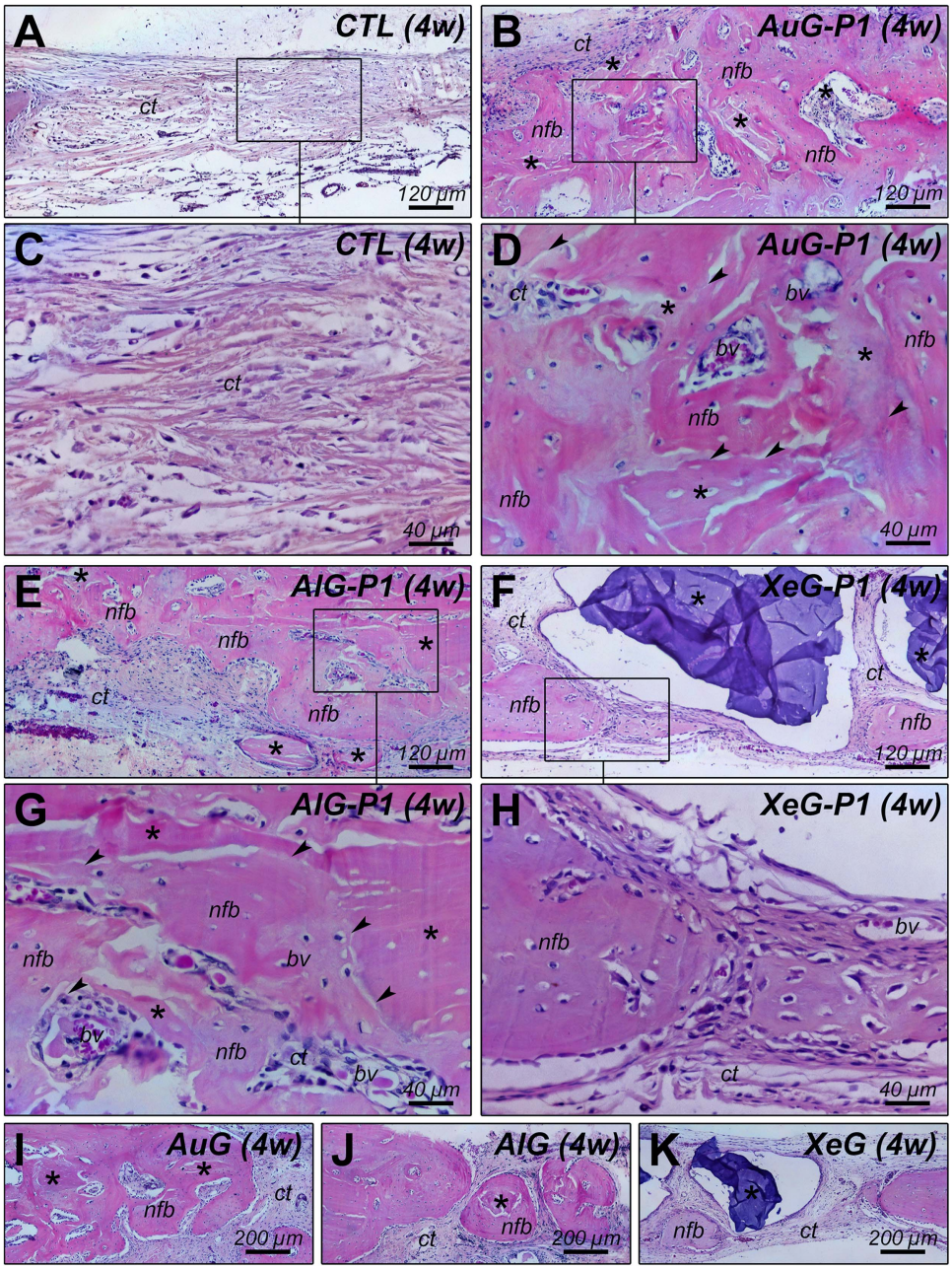

Figure 1. Histological appearance of the center of the bone defect at 4 weeks postoperative. Photomicrographs showing the tissues that filled the bone defect area in CTL (A) and (C), AuG–F1 (B) and (D), AlG–F1 (E) and (G), XeG–F1 (F) and (H), AuG (I), AlG (J) and XeG (K). Abbreviations and symbols: asterisks, remaining bone graft; bv, blood vessels, connective tissue; nfb, neoformed bone; black arrows, boundary between new bone and remaining bone graft. Original magnification: (A), (B), (E), (F), (I), (J), (K) 100×; (C), (D), (G), (H) 400×. Scale bars: (A), (B), (E), (F) 120 μm; (C), (D), (G), (H) 40 μm; (I), (J), (K) 200 μm. Staining: (H) & (E).

(23.39 ± 8.23) group proved to be different only to AuG–F1 and did not differ from the other groups (figure 3(B)).

3.3. Immunohistochemical analysis: analysis of BMP-2

3.3.1. 4-week period

The result for BMP-2 has shown that the AuG–F1 and AlG–F1 groups had higher immunostaining for this protein when compared with the CTL group with statistical differences of $p < 0.05$ (figures 4(A), (C)–(E)).

3.3.2. 6-week period

The data showed that at 6 weeks, the AuG, AuG–F1 and AlG–F1 groups significantly increased BMP-2 immunostaining with a statistical difference to the CTL and F1 groups of $p < 0.01$ and $p < 0.05$ respectively (figure 4(B)).

3.4. OPN analysis

3.4.1. 4-week period

At 4 weeks, the AuG–F1 and AlG–F1 groups presented immunostaining superior to the CTL group with a

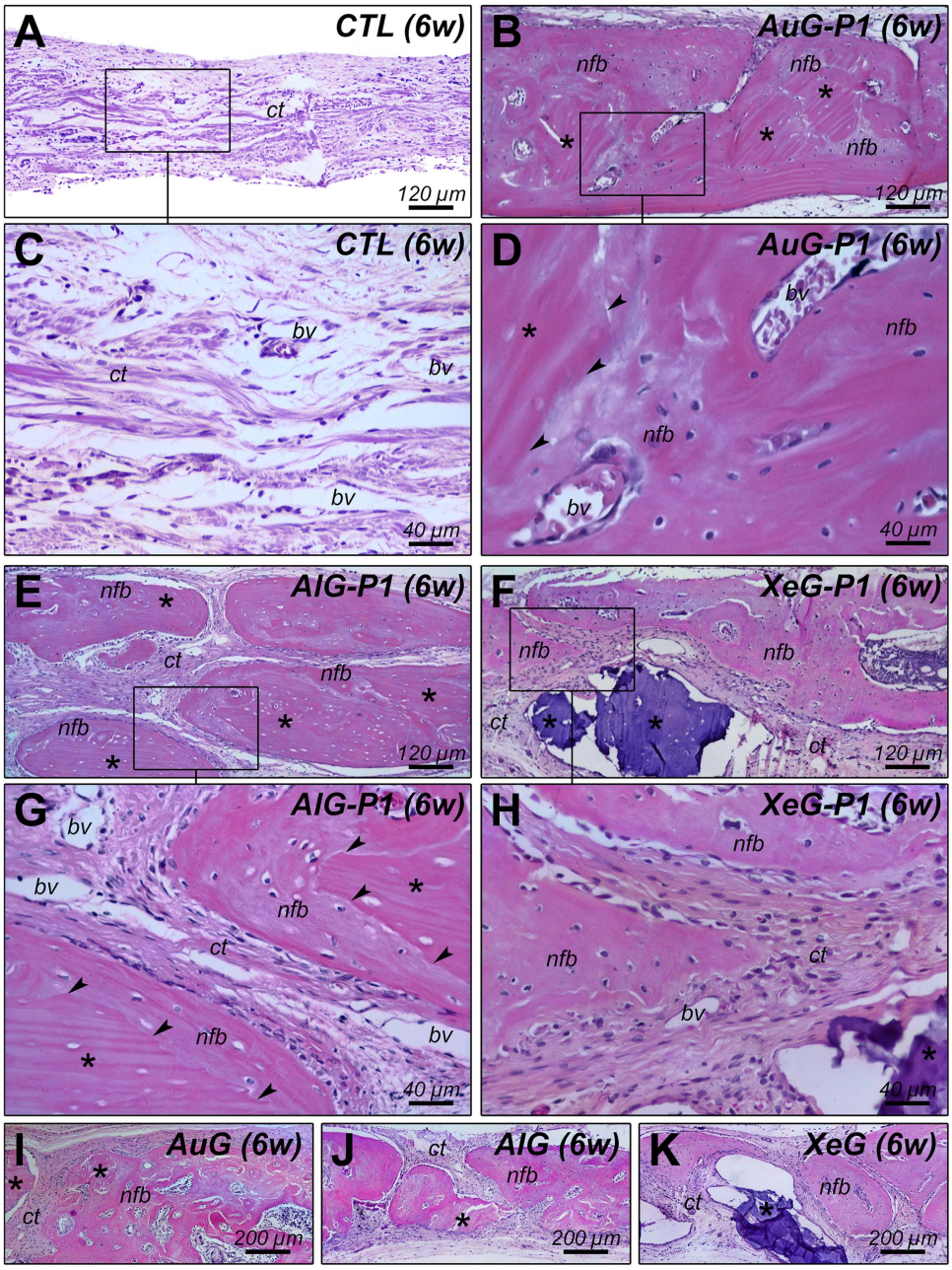

Figure 2. Histological appearance of the center of the bone defect at 6 weeks postoperative. Photomicrographs showing the tissues that filled the bone defect area in CTL (A) and (C), AuG–F1 (B) and (D), AlG–F1 (E) and (G), XeG–F1 (F) and (H), AuG (I), AlG (J) and XeG (K). Abbreviations and symbols: asterisks, remaining bone graft; bv, blood vessels, connective tissue; nfb, neoformed bone; black arrows, boundary between new bone and remaining bone graft. Original magnification: (A), (B), (E), (F), (I), (J), (K) 100x; (C), (D), (G), (H) 400x. Scale bars: (A), (B), (E), (F) 120 μm; (C), (D), (G), (H) 40 μm; (I), (J), (K) 200 μm. Staining: (H) & (E).

statistical difference of $p < 0.05$. The other groups did not differ from the control and AuG–F1 and AlG–F1 groups (figure 4(F)).

3.4.2. 6-week period

At 6 weeks, the AuG–F1 group presented immunostaining superior to the CTL and F1 groups with a statistical difference of $p < 0.05$. The other groups did not differ from the control (figures 4(G)–(J)).

3.5. OCN analysis

3.5.1. 4-week period

Data showed superior immunostaining for OCN in the AuG–F1 and AlG–F1 groups with a statistical difference to the CTL of $p < 0.05$. The other groups did not differ statistically to any group (figure 4(K)).

3.5.2. 6-week period

Results showed that the AuG–F1, AlG–F1 and XeG–F1 groups differed statistically from the CTL group

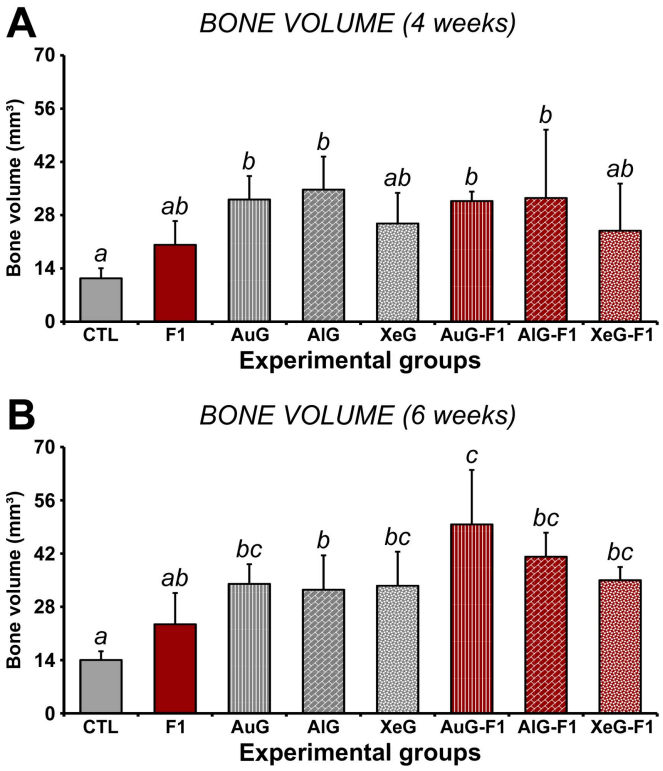

Figure 3. Graphics showing the mean and standard deviations of bone volume (in mm^3) in the different experimental groups at 4 (A) and 6 (B) weeks postoperative ($n = 7$). Letters indicate statistical differences (same letter, no differences; different letters, significant differences).

($p < 0.01$, $p < 0.05$ and $p < 0.05$ respectively), presenting more immunostaining for OCN. The other groups did not differ statistically to any group (figures 4(L)–(O)).

3.6. VEGF analysis

3.6.1. 4-week period

There was no statistical difference between the treatments for this protein in this period (figures 5(A), (C)–(E)).

3.6.2. 6-week period

There was no statistical difference between treatments for this protein in this period (figure 5(B)).

3.7. VEGF-R2 analysis

3.7.1. 4-week period

Statistical differences for the different treatments were not found in this period (figures 5(F), (H)–(J)).

3.7.2. 6-week period

Statistical differences for the different treatments were not found in this period (figure 5(G)).

3.8. CD31 Analysis

3.8.1. 4-week period

Data showed that the AuG, AlG, AuG–F1, AlG–F1, XeG–F1 and F1 groups differed statistically from the CTL group with $p < 0.01$, and only the XeG group showed immunostaining for CD31, similar to CTL (figure 5(K)).

3.8.2. 6-week period

The AuG–F1 and AlG–F1 groups presented statistical differences to the CTL group with $p < 0.01$, showing higher immunostaining for CD31 in this period (figures 5(L)–(O)).

3.9. Analysis of TRAP-positive cells

3.9.1. 4-week period

The result for the TRAP analysis demonstrated that the XeG–F1 group had a higher number of TRAP positive cells compared with the other groups, with a statistical difference of $p < 0.001$. The AlG–F1 group also demonstrated the presence of a greater number of cells compared to the CTL group and AuG with $p < 0.05$. The other groups (AuG, AlG, XeG, AuG–F1, and F1) were similar to each other and to the control (figures 6(A), (C)–(K)).

3.9.2. 6-week period

The results showed that in this period, the XeG, AlG–F1 and XeG–F1 groups showed a higher number of TRAP positive cells with statistically significant differences to the CTL ($p < 0.001$, $p < 0.01$, $p < 0.001$) respectively. It was noticed that the AuG, AlG and CTL groups were the groups with smaller numbers of cells found (figure 6(B)).

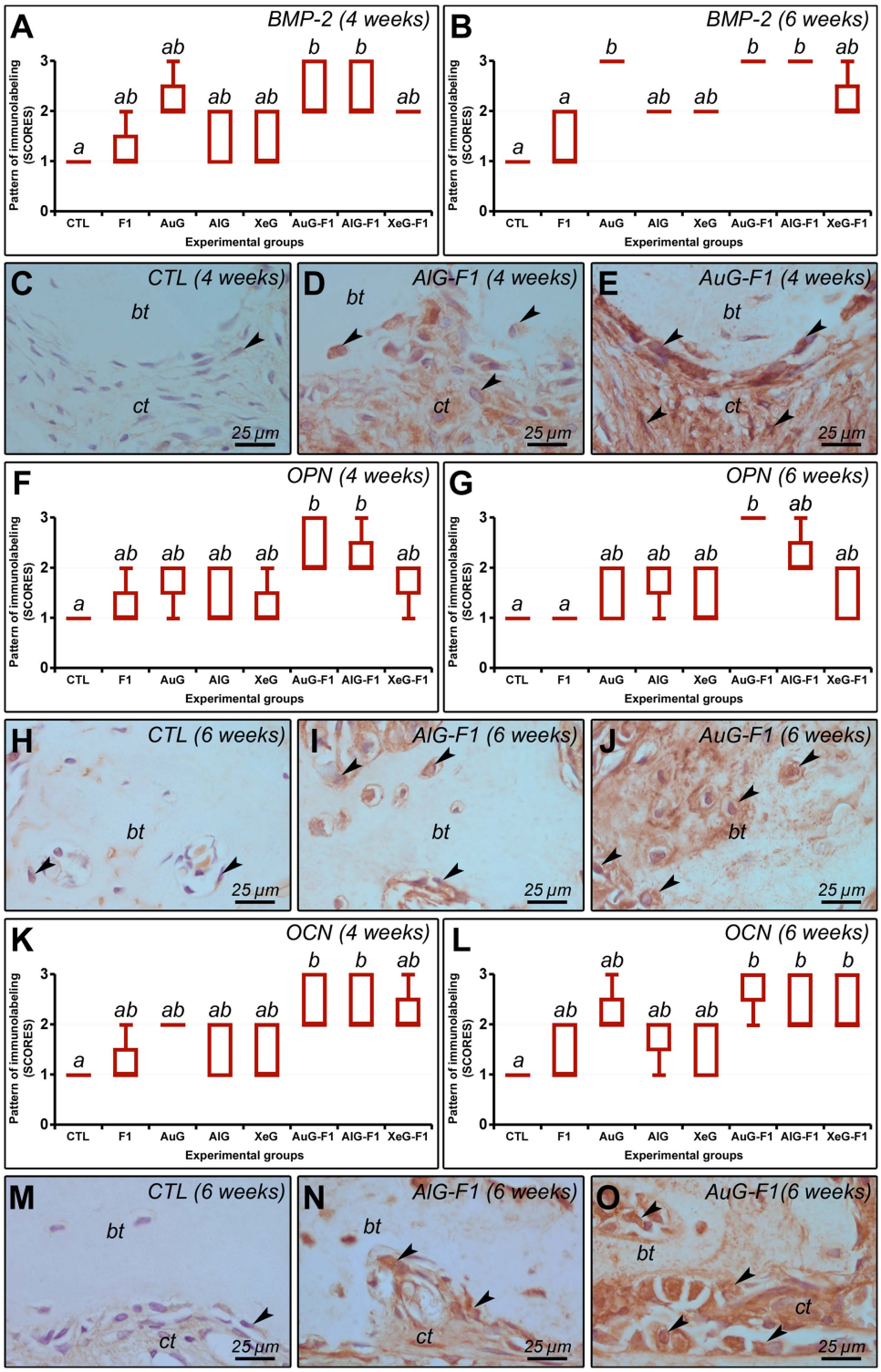

Figure 4. Immunolabeling for BMP-2, OPN and OCN in the critical bone defect of the calvaria in the different experimental groups and periods. (A)–(B), F)–(G), (K)–(L) Graphics showing the median and interquartile deviation of immunolabeling for BMP-2 (A)–(B), OPN (F)–(G) and OCN (K)–(L) in the experimental groups at 4 (A), (F) and (K) and 6 (B), (G) and (L) weeks postoperative. (C)–(E), (H)–(J), (M)–(O) Photomicrographs showing the immunolabeling for BMP-2 (C)–(E), OPN (H)–(J) and OCN (M)–(O) in CTL, AlG–F1 and AuG–F1 groups. Abbreviations and symbols: ct, connective tissue; bt, bone tissue; black arrows, immunolabeling cells. Original magnification: (C)–(E), (H)–(J) and (M)–(O) 1000×. Scale bars: (C)–(E), (H)–(J) and (M)–(O) 25 μm. Counterstaining: Harris Hematoxylin.

3.10. Result of zymographic analysis

3.10.1. Result of proMMP-9 analysis in the 4-week period

Statistical analysis showed that at 4 weeks, the groups that received the graft associated with F1 showed gelatinolytic activity of proMMP-9 higher than the other groups ($p < 0.05$). However, F1 applied alone was not able to increase these values and was not statistically different from the control group and the group that received only the graft. It is observed that

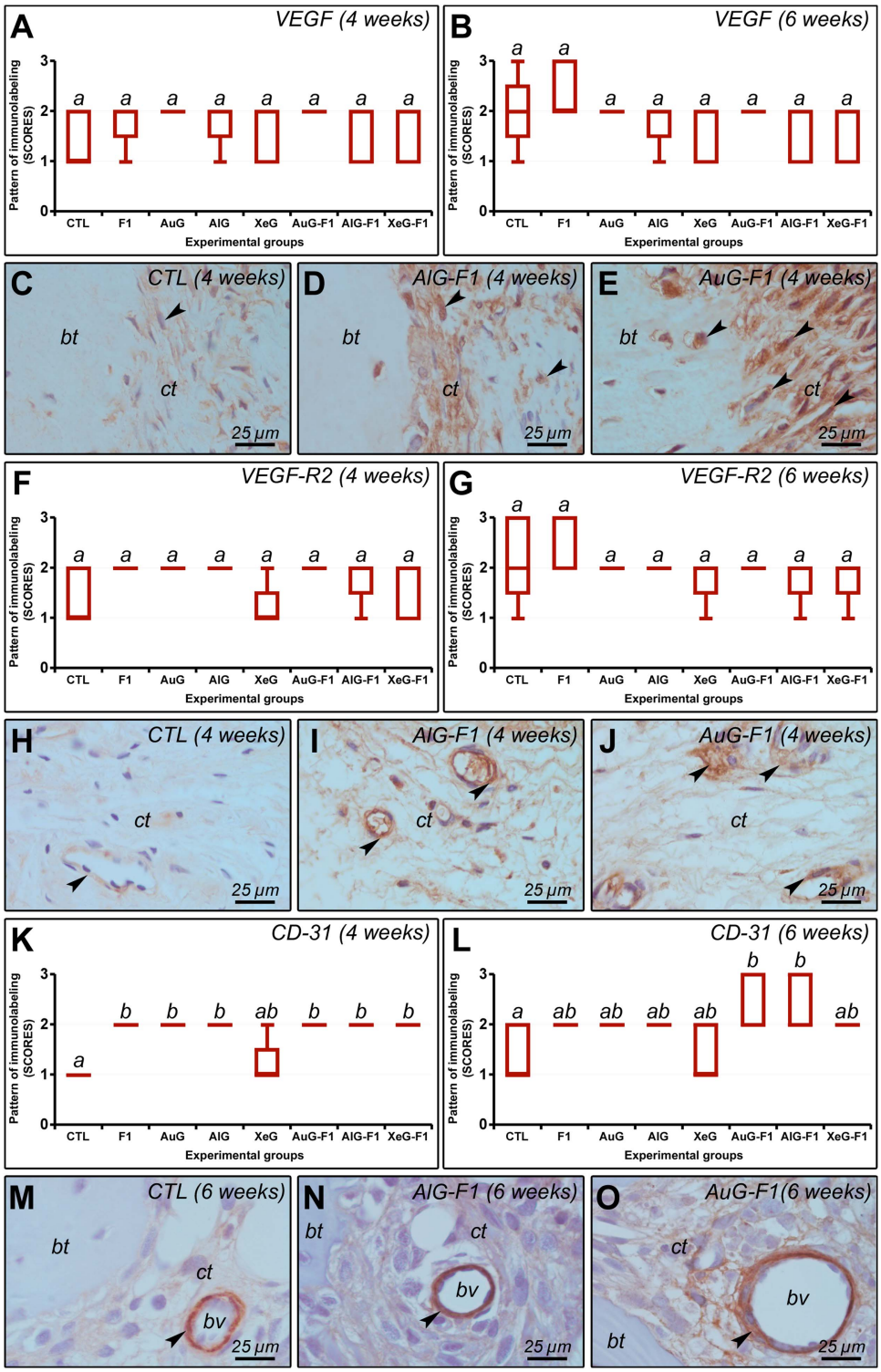

Figure 5. Immunolabeling for VEGF, VEGF-R2 and CD-31 in the bone defect of the calvaria of different experimental groups and periods. (A)–(B), (F)–(G), (K)–(L) Graphics showing the median and interquartile deviation of the pattern of immunolabeling for VEGF (A–B), VEGF-R2 (F–G) and CD-31 (K–L) in the experimental groups at 4 (A), (F) and (K) and 6 (B), (G) and (L) weeks postoperative. (C)–(E), (H)–(J), (M)–(O) Photomicrographs showing the immunolabeling for VEGF (C)–(E), VEGF-R2 (H)–(J) and CD-31 (M)–(O) in CTL, AlG–F1 and AuG–F1 groups. Abbreviations and symbols: ct, connective tissue; bt, bone tissue; bv, blood vessels; black arrows, immunolabeling cells. Original magnification: (C)–(E), (H)–(J) and (M)–(O) 1000×. Scale bars: (C)–(E), (H)–(J) and (M)–(O) 25 μm. Counterstaining: Harris Hematoxylin.

the graft and F1 (applied alone) are not able to affect these enzymatic levels; however, the association of the different grafts and the protein F1 raises these values (figures 7(A) and (B)).

3.10.2. Result of proMMP-9 analysis in the 6-week period

All groups except AuG–F1 were statistically similar to the control ($p < 0.01$). It was noted that the AuG–F1 group

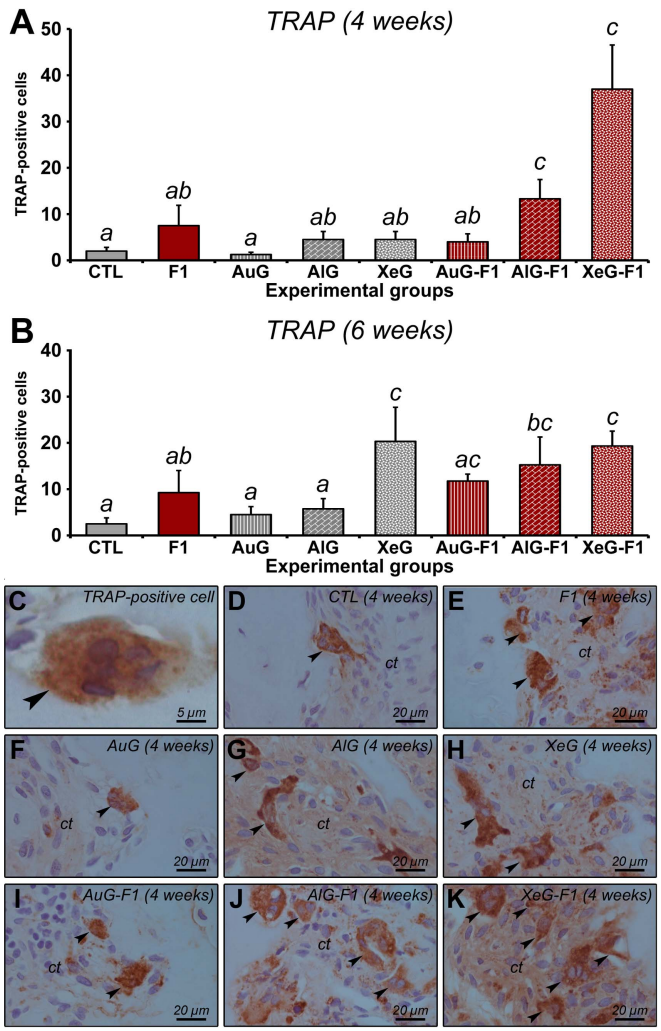

Figure 6. Immunolabeling for TRAP in the critical bone defect of the calvaria in the different experimental groups and periods. (A)–(B) Graphics showing the mean and standard deviations of the number of TRAP positive cells in the experimental groups at 4 (A) and 6 (B) weeks postoperative. (C)–(K) Photomicrographs showing the TRAP positive cell (C) in CTL (D), F1 (E), AuG (F), AlG (G), XeG (H), AuG–F1 (I), AlG–F1 (J) and XeG–F1 (K) groups at 4 weeks postoperative. Abbreviations and symbols: ct, connective tissue; black arrows, TRAP-positive cells. Original magnification: (C) 4000x, (D)–(K) 1000×. Scale bars: (C) 5 μm, (D)–(K) 20 μm. Counter-staining: Harris Hematoxylin.

showed the highest gelatinolytic activity for proMMP-9, and did not differ statistically from the other groups which received F1 alone or associated with different grafts. These AlG–F1, F1 and XeG–F1 groups were intermediate, with gelatinolytic activity without statistical differences for any group (figures 7(A) and (B)).

3.10.3. Result of MMP-9 analysis in the 4-week period

The AuG, AlG, XeG, AlG–F1 and F1 groups did not differ statistically from the control. The AuG–F1 group had the highest enzymatic value for MMP-9 and differed statistically from groups AuG, AlG, CTL ($p < 0.01$) and XeG $p < 0.05$ respectively. The AlG–F1, XeG–F1 and F1 groups were shown to be intermediate, and did not differ statistically from any group (figures 7(A) and (B)).

3.10.4. Result of MMP-9 analysis in the 6-week period

The results showed no statistical difference in relation to the groups. However, it was noted that the groups that received the graft and F1 showed a tendency of increased MMP-9 levels (figures 7(A) and (B)).

3.10.5. ProMMP-2 analysis results (4 weeks)

For zymographic analysis of proMMP-2 at 4 weeks, AlG–F1, XeG–F1 and the F1 groups were similar to each other but statistically different from the CTL ($p < 0.05$ and $p < 0.01$ respectively), presenting gelatinolytic activity superior to the control. The AuG, AlG, XeG, and AuG–F1 groups were not statistically different to the CTL (figures 7(A) and (C)).

3.10.6. Results of zymographic analysis of proMMP-2 (6 weeks)

AuG–F1, AlG–F1 XeG–F1 and F1 groups exhibited higher gelatinolytic activity for proMMP-2, the last four groups being statistically different to CTL, AuG and AlG ($p < 0.05$). The XeG showed no statistical difference between the groups (figures 7(A) and (C)).

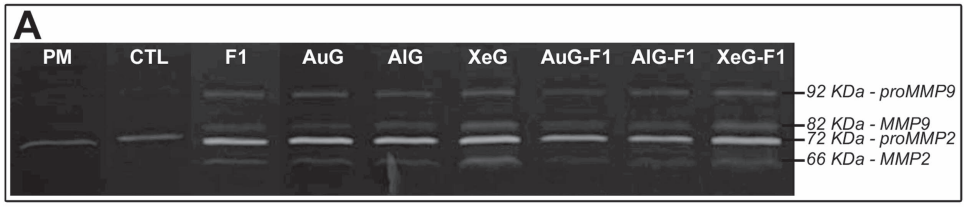

B

Groups	proMMP9 (4 weeks)	MMP9 (4 weeks)	proMMP9 (6 weeks)	MMP9 (6 weeks)
CTL	1.08 ± 0.24 ^{ab}	1.00 ± 0.06 ^{a}	1.08 ± 0.26 ^{a}	0.93 ± 0.18 ^{a}
F1	4.99 ± 3.52 ^{ac}	2.79 ± 0.77 ^{ab}	17.97 ± 15.69 ^{ab}	2.71 ± 1.26 ^{a}
AuG	4.17 ± 0.92 ^{ac}	1.03 ± 0.23 ^{a}	4.02 ± 0.30 ^{a}	0.77 ± 0.12 ^{a}
AlG	4.69 ± 0.93 ^{ac}	1.14 ± 0.04 ^{ac}	3.91 ± 1.46 ^{a}	0.83 ± 0.15 ^{a}
XeG	5.21 ± 0.82 ^{ac}	1.31 ± 0.39 ^{ac}	5.04 ± 1.33 ^{a}	1.38 ± 0.26 ^{a}
AuG-F1	14.33 ± 7.59 ^{bcd}	3.46 ± 2.03 ^{b}	31.27 ± 18.25 ^{b}	2.21 ± 0.63 ^{a}
AlG-F1	15.49 ± 10.60 ^{cd}	1.85 ± 0.73 ^{ab}	10.34 ± 16.93 ^{ab}	2.71 ± 1.52 ^{a}
XeG-F1	19.44 ± 15.25 ^{d}	2.98 ± 1.15 ^{bc}	11.07 ± 9.09 ^{ab}	2.62 ± 1.62 ^{a}

C

Groups	proMMP2 (4 weeks)	MMP2 (4 weeks)	proMMP2 (6 weeks)	MMP2 (6 weeks)
CTL	41.36 ± 2.37 ^{a}	42.24 ± 3.76 ^{a}	43.60 ± 8.79 ^{ab}	40.80 ± 7.67 ^{ab}
F1	85.76 ± 11.83 ^{bc}	50.45 ± 14.47 ^{a}	82.41 ± 14.99 ^{c}	50.48 ± 19.12 ^{ab}
AuG	43.20 ± 6.11 ^{a}	46.88 ± 7.14 ^{a}	37.44 ± 4.43 ^{ab}	38.48 ± 6.68 ^{ab}
AlG	47.36 ± 7.99 ^{ad}	44.64 ± 10.50 ^{a}	32.88 ± 6.37 ^{ab}	33.36 ± 5.83 ^{a}
XeG	60.56 ± 12.06 ^{acd}	52.32 ± 10.55 ^{a}	69.20 ± 11.06 ^{bc}	61.36 ± 5.54 ^{b}
AuG-F1	70.36 ± 36.61 ^{ab}	53.40 ± 17.48 ^{a}	77.29 ± 15.92 ^{c}	41.09 ± 15.31 ^{ab}
AlG-F1	77.75 ± 16.32 ^{bd}	36.57 ± 11.91 ^{a}	86.20 ± 15.08 ^{c}	32.41 ± 11.92 ^{a}
XeG-F1	89.25 ± 10.72 ^{bc}	56.09 ± 8.06 ^{a}	87.01 ± 18.85 ^{c}	38.11 ± 13.03 ^{ab}

Figure 7. Zymographic gel analysis (A). Tables showing the mean and standard deviations of zymographic analysis for proMMP-9, MMP-9 at 4 and 6 weeks postoperative (B), and for proMMP-2 and MMP-2 4 and 6 weeks postoperative (C).

3.10.7. Result of MMP-2 analysis (4 weeks)

In the 4-week period, gelatinolytic activity of MMP-2 was not statistically different for the different treatments (figures 7(A) and (C)).

3.10.8. Result of zymographic analysis of MMP-2 (6 weeks)

AlG and AlG–F1 groups differed statistically from XeG ($p < 0.05$ and 0.01 respectively); however, no treatments showed changes of gelatinolytic activity in relation to the control (figures 7(A) and (C)).

4. Discussion

The effects of F1 protein associated with different types of grafts were analyzed in our work, and the benefits related to its use, as well as its disadvantages, have been discussed and described in the literature, but the association of F1 and its effects on bone healing are still unknown.

This protein has been shown to have important biological properties, such as neoangiogenesis activity, cell adhesion, and extracellular matrix formation, and is already being used for different medical purposes [10, 23–26]. The bone repair process is dependent on several factors, including the formation of blood vessels and orchestrated activity of osteoblasts and osteoclasts, so the stimulation of angiogenesis is a promising approach for bone formation.

The results for these experimental groups after a 4-week waiting period by stereological and histological analysis showed that the AuG, AlG, AuG–F1 and AlG–F1 groups showed superior bone formation compared to the control group with $p < 0.05$. Histologically, it was possible to observe the presence of bone tissue at the edges of the surgical wound advancing considerably toward the defect center. In the 6-week period, all groups except F1 showed statistically significant differences with higher values of bone neoformation compared to the control.

Corroborating these results, other studies showed that autograft and allograft are effective in bone neoformation, and are more biocompatible [27–29]. Our work has shown that such grafts increase bone formation compared to the control group and a combination of these grafts with F1 protein increases bone neoformation after 6 weeks of treatment; however, compared to autograft and allograft, this difference was not observed.

The TRAP cell analysis showed that after 4 weeks, the XeG–F1 and AlG–F1 groups had a higher number of immunostained cells, statistically differing from the AuG and CTL groups. When comparing the XeG and XeG–F1 groups, there was an increase in the number of those immunostained cells of the second group's cells compared to the first, showing the effect of F1 protein when combined with a heterologous graft, acceleration of osteoclastogenesis and activation of osteoclasts observed histologically by the active process of bone resorption in these groups. This infers that the lower bone formation of the XeG group is probably due to a higher resorption, precisely because it is a greater heterogeneity graft showing a greater number of osteoclasts and resorptive gaps observed by TRAP. In the XeG–F1 group, we noted by TRAP analysis that there was also an increase in these cells. However, unlike the XeG group, we observed larger areas of bone apposition to the resorptive gaps, showing the active process of bone remodeling, and these findings are well established in the literature [30–32]. The literature mentions that a higher osteoclast presence on the bone during the bone remodeling is an indication of an effective bone remodeling evolving osteoclast [32]; due to this, our findings show that the XeG group had a higher TRAP-labeling in 6 weeks (figure 6(B)), statistically similar to the XeG–F1. These results suggest that the XeG group have a later recruitment of cell osteoclastogenics during the bone remodeling without interfering with bone neoformation. Thus we can see that F1 seems to have a greater impact on osteoclastogenesis because it is another exogenous component applied to the bone defect, and, especially at 6 weeks, increased bone resorption followed later with the process of remodeling, forming and affixing newly formed bone tissue in these groups observed by histological analysis.

As is known for proper bone healing, a series of biological events must occur from the clot formation, and for this, important bone, vascular, and cell growth factors are necessary. In order to analyze and understand the behavior of these factors in the treatment employed, some of these markers were quantified.

The bone markers BMP-2, OCN and OPN are shown to increase in AuG–F1 with significant differences to the control after 4 and 6 weeks. ALG–F1 also demonstrated an increase of BMP-2, OCN and OPN; however, in the 6-week period, OPN did not differ statistically from the control group (figure 4). The XeG–F1 group after 6 weeks also demonstrated a significant increase for this bone marker. These results suggest that the allograft and autograft associated with F1 may be able to increase the stimulation and mineralization of osteoblast and osteoclast adhesion on the surface of the bone matrix associated mainly with these grafts, improving the repair of the bone defect. Application of the grafts and F1 showed a tendency to increase these bone markers, but without statistical differences between the groups and the control, except for AuG to BMP-2 and XeG–F1 to OCN after 6 weeks, thus also interfering with bone repair, and leading to increased bone neoformation, as observed in the stereological analysis.

Analyzing the CD31, VEGF, and VEGF-R2 angiogenic factors, our results showed that all these factors were moderately present in all groups, with the CD31 marker showing a high standard of immunostaining for groups AuG–F1 and ALG–F1 after 6 weeks. This leads us to suggest that the angiogenic factors are stimulated in the presence of different types of graft and can rise in association with the F1 protein with autogenous and allogenous bone grafts for CD31 identification after 6 weeks. These results are consistent with the histological analysis that demonstrated neoangiogenesis in all groups. However, for the autograft and allograft groups associated or not with the F1 protein, many blood vessels, inflammatory cells and the presence of organized bone tissue with few bone marrow spaces and trabeculae were observed advancing completely to the center of the defect.

Another important factor in the bone repair process studied in our work is the MMPs. These are responsible for the degradation of the extracellular matrix, expressed in physiological and pathological processes, and are related to inflammatory processes that act on cartilage and bone remodeling, and angiogenesis in bone healing [33]. Our study analyzed the gelatinolytic activity of MMP-2 and MMP-9. MMP-2 is a collagenase highly expressed by fibroblasts, endothelial and epithelial cells, secreted in the form of proMMP-2 responsible for cleaving collagen, laminin, elastin, fibronectin and proteoglycans [29, 33]. MMP-9 is another collagenase secreted in the form of proMMP-9 expressed by macrophages, keratinocytes and multinucleated osteoclasts in bone resorption [34–36]. These enzymes were analyzed by zymographic analysis, and the results for proMMP-2 at 4 weeks showed that the control had lower gelatinolytic activity of this proenzyme, followed by the AuG, AlG and XeG, AuG–F1, AlG–F1, F1 and XeG–F1 groups. It was noted that the same behavior was observed in the groups after graft association with the F1 protein, which rose consecutively. This demonstrates that, in particular, the AlG–F1, XeG–F1 and F1 groups had higher levels of proMMP-2 when compared to the control. These results lead us to associate the lower compatibility between the graft and 'receptor site' with the higher level of this proenzyme (proMMP-2). Moreover, it is possible to associate the application of F1 with these increased enzymatic levels. At 6 weeks, this proenzyme (proMMP-2) also showed the same pattern found at 4 weeks; however, the AuG–F1, AlG–F1, XeG–F1 and F1 groups were hitherto similar to each other, but differed from the control, and therefore the AuG, AlG and XeG groups did not differ from the control group.

MMP-2 at 4 weeks showed no change in gelatinolytic activity for the different treatments; however, at 6

weeks, it was observed that the XeG group showed the highest gelatinolytic activity for the protein when compared to the AlG and AlG–F1 groups, and the other groups were similar to the control. This enzyme is found in low concentrations in healthy bone and increases in the early stages of the bone healing process, with its peak expression between the third and fourth week; its reduction occurs late and its presence is correlated with the appropriate repair process and bone remodeling, and its absence would lead to a delay in this process [37, 38].

Our results showed that proMMP-2 and MMP-2 are more concentrated in the F1 plus graft groups, mainly linked to the heterologous graft. This may be a result of this graft requiring more time to be reabsorbed and integrated. However, the F1 that was shown to augment these enzyme levels when applied in isolation or associated with other grafts leads us to suggest that this protein alters the local inflammatory response, increasing the catabolism of this region. This is because, when it comes to more than one exogenous component, adding to the surgical defect induces increased production of these metalloproteinases in the degradation of the extracellular matrix, and thus increases these local enzymatic levels. However, this increase of catabolism caused by the addition of F1 does not affect anabolism in the bone repair process, and viewing the results found in stereologic analysis showed that bone neoformation in these groups was similar or slightly higher than the groups not added with this protein.

The proMMP-9 at 4 weeks showed higher levels when the grafts were associated with F1 protein and were significantly different from the control; in isolation, this protein did not change this result. At 6 weeks, we observed the same pattern; however, only the AuG–F1 group remained at these high levels and different to the control group. MMP-9 analyzed at 4 weeks showed AuG–F1 with levels statistically different from the control of this enzyme. An increasing trend was noticed in this enzyme associated with the graft plus F1 groups (F1, AlG–F1 and XeG–F1) with no difference to the control. At 6 weeks, there was no statistical difference for the different treatments.

The proMMP-9 and MMP-9 are expressed in inflammatory cells, and mesenchymal stem cells are related to the repair process, and are expressed in early and late stages of repair [39, 40]. Our results corroborate the literature and likewise demonstrate that the levels of enzymes and proenzymes remained constant in all groups over time. This is because MMP-9 is associated with the inflammatory response modulation process particularly associated with its expression by osteoclasts for reabsorption and replacement of the graft by newly formed bone [41]. Since MMP-9 has greater expression in the graft plus F1 groups, we can correlate this increase in the enzymatic level to the increase of the number of osteoclasts seen in TRAP cell analysis. This association between graft and F1 has been shown to increase the cell number of osteoclasts which suggests larger bone remodeling in these groups.

Bone grafts associated or not with F1 protein demonstrated increased bone formation and osteogenic and angiogenic factors. The enzymatic factors for MMP-2 and 9 were influenced by F1 in both experimental periods. Therefore, further studies should be carried out to clarify the effects of this protein on bone repair, especially involving other experimental animal models and different time periods.

Acknowledgments

The authors are grateful to FAPESP for financial support, processes N. 2012/03310-8 and 2012/22532-1. The authors are very grateful for the protein supply and support provided by Professor Joaquim Coutinho-Netto, *in memoriam.*

Declaration of Interest

The authors declare that they have no competing financial interests. The authors declare that they have no conflict of interest.

ORCID iDs

Fellipe A T de Figueiredo https://orcid.org/0000-0001-9924-9751
João Paulo Mardegan Issa https://orcid.org/0000-0002-1056-0795

References

[1] Abrahams J J, Hayt M W and Rock R 2000 Sinus lift procedure of the maxilla in patients with inadequate bone for dental implants: radiographic appearance *AJR Am. J. Roentgenol.* **174** 1289–92
[2] Graziani F, Donos N, Needleman I, Gabriele M and Tonetti M 2004 Comparison of implant survival following sinus floor augmentation procedures with implants placed in pristine posterior maxillary bone: a systematic review *Clin. Oral Implants Res.* **15** 677–82
[3] Yildirim M, Spiekermann H, Biesterfeld S and Edelhoff D 2000 Maxillary sinus augmentation using xenogenic bone substitute material Bio-Oss in combination with venous blood. A histologic and histomorphometric study in humans *Clin. Oral Implants Res.* **11** 217–29
[4] Issa J P *et al* 2010 Evaluation of rhBMP-2 and natural latex as potential osteogenic proteins in critical size defects by histomorphometric methods *Anat. Rec. (Hoboken)* **293** 794–801
[5] Nascimento R M, Faita F L, Agostini D L S, Job A E, Guimarães F E G and Bechtold I H 2014 Production and characterization of natural rubber-Ca/P blends for biomedical purposes *Mater. Sci. Eng. C* **39** 29–34
[6] Dias F J *et al* 2015 Morphometric and high resolution scanning electron microscopy analysis of low-level laser therapy and latex protein (Hevea brasiliensis) administration following a crush injury of the sciatic nerve in rats *J. Neurol. Sci.* **349** 129–37
[7] Machado E G *et al* 2015 A new heterologous fibrin sealant as scaffold to recombinant human bone morphogenetic protein-2 (rhBMP-2) and natural latex proteins for the repair of tibial bone defects *Acta Histochem.* **117** 288–96

[8] Mrue F, Netto J C, Ceneviva R, Lachat J J, Thomazini J A and Tambelini H 2004 Evaluation of the biocompatibility of a new biomembrane *Mater. Res.* **7** 277–83
[9] Andrade T A M, Iyer A, Das P K, Foss N T, Garcia S B, Coutinho-Netto J and Frade M A C 2011 The inflammatory stimulus of a natural latex biomembrane improves healing in mice *Braz. J. Med. Biol. Res.* **44** 1036–47
[10] Frade M A, Valverde R V, de Assis R V, Coutinho-Netto J and Foss N T 2001 Chronic phlebopathic cutaneous ulcer: a therapeutic proposal *Int. J. Dermatol.* **40** 238–40
[11] Raulf M 2014 The latex story *Chem. Immunol. Allergy* **100** 248–55
[12] Vandenplas O *et al* 2016 The role of allergen components for the diagnosis of latex-induced occupational asthma *Allergy* **71** 840–9
[13] Wu M, McIntosh J and Liu J 2016 Current prevalence rate of latex allergy: why it remains a problem? *J. Occup. Health* **58** 138–44
[14] Caballero M L and Quirce S 2015 Identification and practical management of latex allergy in occupational settings *Expert. Rev. Clin. Immunol.* **11** 977–92
[15] Balabanian C A, Coutinho-Netto J, Lamano-Carvalho T L, Lacerda S A and Brentegani L G 2006 Biocompatibility of natural latex implanted into dental alveolus of rats *J. Oral. Sci.* **48** 201–5
[16] Frade M A, Coutinho Netto J, Gomes F G, Mazzucato E L, Andrade T A and Foss N T 2011 Natural-biomembrane dressing and hypersensitivity *An. Bras. Dermatol.* **86** 885–91
[17] Frade M A, Assis R V, Coutinho Netto J, Andrade T A and Foss N T 2012 The vegetal biomembrane in the healing of chronic venous ulcers *An. Bras. Dermatol.* **87** 45–51
[18] Ereno C *et al* 2010 Latex use as an occlusive membrane for guided bone regeneration *J. Biomed. Mater. Res.* A **95** 932–9
[19] Mendonca R J, Mauricio V B, Teixeira Lde B, Lachat J J and Coutinho-Netto J 2010 Increased vascular permeability, angiogenesis and wound healing induced by the serum of natural latex of the rubber tree Hevea brasiliensis *Phytother. Res.* **24** 764–8
[20] Ferreira M, Mendonça R J, Coutinho-Netto J and Mulato M 2009 Angiogenic properties of natural rubber latex biomembranes and the serum fraction of Hevea brasiliensis *Braz. J. Phys.* **39** 564–9
[21] Gosain A K *et al* 2000 Osteogenesis in cranial defects: reassessment of the concept of critical size and the expression of TGF-beta isoforms *Plast. Reconstr. Surg.* **106** 360–71
[22] Faria P E, Okamoto R, Bonilha-Neto R M, Xavier S P, Santos A C and Salata L A 2008 Immunohistochemical, tomographic and histological study on onlay iliac grafts remodeling *Clin. Oral Implants Res.* **19** 393–401
[23] Oliveira J A A D, Hyppolito MA, Coutinho Netto J and Mrué F 2003 Miringoplastia com a utilização de um novo material biossintético *Revista Brasileira de Otorrinolaringologia* **69** 649–55
[24] Brandão M L, Coutinho Netto J, Thomazini J A, Lachat J J, Muglia V F and Piccinato C E 2007 Prótese vascular derivada do látex *Jornal Vascular Brasileiro* **6** 130–41
[25] Silva L S D, RMM C and Rosa C D O B 2013 Estratégias de promoção da saúde e prevenção primária para enfrentamento das doenças crônicas: revisão sistemática *Revista Panamericana de Salud Pública* **34** 343–50
[26] Pinho E C C M D, Sousa S J D F E, Schaud F, Lachat J-J and Coutinho-Netto J 2004 Uso experimental da biomembrana de látex na reconstrução conjuntival *Arquivos Brasileiros de Oftalmologia* **67** 27–32
[27] Rocha F S, Ramos L M A, Batista J D, Zanetta-Barbosa D and Dechichi P 2011 Enxerto bovino orgânico associado ao PRP em calvária de coelhos *Arquivos Internacionais de Otorrinolaringologia* **15** 208–13
[28] Xavier S P, Silva E R, Kahn A, Chaushu L and Chaushu G 2015 Maxillary sinus grafting with autograft versus fresh-frozen allograft: a split-mouth evaluation of bone volume dynamics *Int. J. Oral Maxillofacial Implants* **30** 1137–42
[29] Sbordone C, Toti P, Guidetti F, Califano L, Pannone G and Sbordone L 2014 Volumetric changes after sinus augmentation using blocks of autogenous iliac bone or freeze-dried allogeneic bone. A non-randomized study *J. Craniomaxillofac. Surg.* **42** 113–8
[30] Galindo-Moreno P *et al* 2011 Effect of anorganic bovine bone to autogenous cortical bone ratio upon bone remodeling patterns following maxillary sinus augmentation *Clin. Oral Implants Res.* **22** 857–64
[31] Gotz W, Gerber T, Michel B, Lossdorfer S, Henkel K O and Heinemann F 2008 Immunohistochemical characterization of nanocrystalline hydroxyapatite silica gel (NanoBone(r)) osteogenesis: a study on biopsies from human jaws *Clin. Oral Implants Res.* **19** 1016–26
[32] Issa J P, Gonzaga M, Kotake B G, de Lucia C, Ervolino E and Iyomasa M 2016 Bone repair of critical size defects treated with autogenic, allogenic, or xenogenic bone grafts alone or in combination with rhBMP-2 *Clin. Oral Implants Res.* **27** 558–66
[33] Behonick D J *et al* 2007 Role of matrix metalloproteinase 13 in both endochondral and intramembranous ossification during skeletal regeneration *PLoS One* **2** e1150
[34] Galasso O, Familiari F, De Gori M and Gasparini G 2012 Recent findings on the role of gelatinases (matrix metalloproteinase-2 and -9) in osteoarthritis *Adv. Orthopedics* **2012** 7
[35] Sternlicht M D and Werb Z 2001 How matrix metalloproteinases regulate cell behavior *Annu. Rev. Cell. Dev. Biol.* **17** 463–516
[36] Reponen P, Sahlberg C, Munaut C, Thesleff I and Tryggvason K 1994 High expression of 92-kD type IV collagenase (gelatinase B) in the osteoclast lineage during mouse development *J. Cell Biol.* **124** 1091–102
[37] Itagaki T, Honma T, Takahashi I, Echigo S and Sasano Y 2008 Quantitative analysis and localization of mRNA transcripts of type I collagen, osteocalcin, MMP 2, MMP 8, and MMP 13 during bone healing in a rat calvarial experimental defect model *Anat. Rec. (Hoboken)* **291** 1038–46
[38] Lieu S *et al* 2011 Impaired remodeling phase of fracture repair in the absence of matrix metalloproteinase-2 *Dis. Model. Mech.* **4** 203–11
[39] Colnot C, Thompson Z, Miclau T, Werb Z and Helms J A 2003 Altered fracture repair in the absence of MMP9 *Development* **130** 4123–33
[40] Wang X *et al* 2013 MMP9 regulates the cellular response to inflammation after skeletal injury *Bone* **52** 111–9
[41] Lu M and Rabie A B 2006 Matrix metalloproteinase-9 regulates graft bone resorption *Angle Orthod* **76** 598–604